THE JOURNAL OF PHYSICAL CHEMISTRY B

Article

pubs.acs.org/JPCB

Polarization Effects of Dielectric Nanoparticles in Aqueous Charge-Asymmetric Electrolytes

Guillermo Iván Guerrero García[†] and Monica Olvera de la Cruz*[,†,‡]

[†]Department of Materials Science and Engineering, and [‡]Department of Chemical and Biological Engineering, Northwestern University, Evanston, Illinois 60208, United States

ABSTRACT: Small nanoparticles, globular proteins, viral capsids, and other nanoscopic biomolecules usually display dielectric properties that are different from those of the medium in which they are dispersed. These dielectric heterogeneities can significantly influence the surrounding ion distribution, which determines the self-assembly and colloidal stability of these nanoparticles in solution. Here, we study the impact of a dielectric discontinuity in the structural and thermodynamic properties of a spherical nanoparticle made of different dielectric materials when it is immersed in a charge-asymmetric 1:z supporting electrolyte. The mean electrostatic potential, integrated charge, and ionic profiles are analyzed as a function of both the salt concentration and the nanoparticle's valence via Monte Carlo simulations and the nonlinear Poisson−Boltzmann theory. We observe that the electrostatic screening and charge neutralization near the surface of a nanoparticle increase when the nanoparticle's dielectric permittivity increases in all instances. For 1:1 salts, this effect is small and the nonlinear Poisson−Boltzmann theory displays a good agreement with simulation results. Nevertheless, significant deviations are displayed by the mean field scheme regarding simulation results in the presence of multivalent ions. In particular, for trivalent counterions we observe that increasing the dielectric permittivity or the valence of the nanoparticle decreases the critical salt concentration at which occurs a sign inversion of the mean electrostatic potential at the Helmholtz plane, which is closely related to the behavior of the ζ potential and the electrophoretic mobility. Moreover, we observe that the phenomenon of surface charge amplification, or the augmenting of the net charge of a nanoparticle by the adsorption of like-charged ions on its surface, can be promoted by polarization effects in weakly charged spherical nanoparticles with low dielectric permittivity.

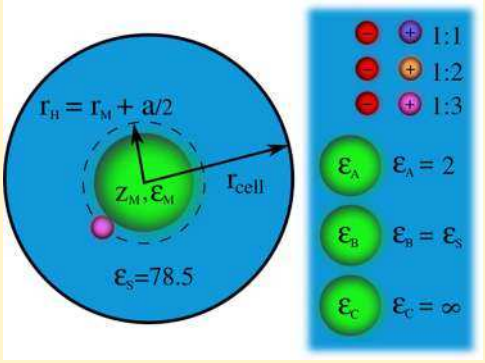

INTRODUCTION

The dielectric properties of charged nanoparticles are in general different from those of the solvent in which they are dissolved. This difference has been used to differentiate experimentally empty virus capsids from similar capsids containing DNA, thus resolving the dielectric constant of single nanoparticles via electrostatic force microscopy.[1] This physical property may be used in a variety of technological applications including label-free detection of the material composition of nanoparticles. Electrostatic force microscopy also has been shown to be a useful tool for determining experimentally the dielectric properties of nonspherical dielectric nanoparticles,[2] as well as the dielectric properties of electrically insulating nanomaterials or the quantum capacitance of conducting materials at the nanoscale.[3] On the other hand, it has been observed experimentally that charged gold nanoparticles in aqueous solutions can self-assemble in chain-like structures in the presence of small concentrations of divalent ions.[4] These nanostructures may be used as building blocks for developing nanoelectronic devices with convenient features. Biological nanocolloids, including lipid bilayers[5−7] and globular proteins,[8] are another class of physical systems in which the dielectric properties at the interior of nanoparticles may be significantly different from those of the surrounding solvent. The presence of dielectric heterogeneities in these small nanoparticles influences the ionic distribution, or the so-called electrical double layer, formed around them, which is known to determine the self-assembly and physical properties of charged nanoparticles in electrolyte solutions.

From a theoretical perspective, important advances have been undertaken since the pioneering work by Onsager and Samaras[9] to model polarization effects in aqueous solutions.[10−13] As a particular example, it has been shown by several studies that image charge effects can drive an attractive net interaction between uncharged walls immersed in an aqueous electrolyte solution in the absence of specific short-range dispersion forces (as van der Waals interactions).[14−17] This may occur if the dielectric constant of the walls is lower than that of the solvent. Physically, this attraction is produced by a depletion of ions near the dielectric discontinuity, producing a lower pressure at short separation distances between the uncharged walls in comparison with the pressure of the electrolyte in bulk. A similar depletion of ions, due mainly to ionic self-image electrostatic interactions, has been

Received: May 7, 2014
Revised: June 13, 2014
Published: June 20, 2014

dx.doi.org/10.1021/jp5045173 | J. Phys. Chem. B 2014, 118, 8854−8862

also observed in computer simulations of charged spherical colloids in the presence of dielectric discontinuities.[18−23] Nevertheless, the experimental measurement of forces between small nanoparticles is significantly more difficult than in the case of their mesoscopic counterpart, that is, colloidal particles with linear dimensions of microns. Fortunately, in both instances it is possible to characterize the electrostatic screening of charged particles via electrophoretic mobility experiments,[24−28] in which an external electric field is applied.[29,30] As a result, the charged colloids reach a terminal velocity that can be used to define the corresponding electrophoretic mobility. This quantity is a useful parameter for characterizing the macroscopic behavior of colloids in solution, including their coagulation and stability regimes. When these colloidal particles move under the action of an electric field, a strongly adsorbed layer of counterions that travels with the colloid defines a slipping or shear plane. The mean electrostatic potential at the slipping or shear plane of the charged colloids is the so-called ζ potential,[30] which can be directly related to the electrophoretic mobility under several approximations.[30−32] The exact location of the ζ potential is generally unknown experimentally, although it has been estimated to be located very near the colloidal surface.[29,30] Conventionally, the location of the ζ potential is associated with the closest approach distance of the ionic species, which is the so-called Helmholtz plane. Thus, the properties of the ζ potential can be inferred from the mean electrostatic potential at the Helmholtz plane as a first approximation.

In this work we study the influence of polarization effects, ion correlations, and excluded volume effects in structural and thermodynamic properties of small charged nanoparticles in 1:z electrolytes. Given the relevance of the electrokinetic behavior of suspended nanoparticles in aqueous solutions,[33−35] we consider nanoparticles made of materials with different dielectric permittivities. Then, we calculate via Monte Carlo simulations the corresponding mean electrostatic potential at the Helmholtz plane for a wide range of electrolyte concentrations. The observed behavior is analyzed in terms of the local charge neutralization produced by the associated ion distribution of multivalent ions. These simulation results are also collated with the nonlinear Poisson−Boltzmann theory in spherical geometry, which is used as a theoretical baseline.

MODEL SYSTEM, SIMULATIONS, AND THEORY

A fixed spherical nanoparticle of radius r_M is immersed in an aqueous primitive model electrolyte enclosed by a spherical hard cell, as shown in Figure 1a. In this approach, the nanoparticle and the ions are represented by hard spheres with point-charges embedded in their centers. The aqueous solvent is approximated by a continuum medium of dielectric constant ε_S = 78.5 at T = 298 K. The material at the interior of the nanoparticle is modeled as a solid continuum medium of dielectric constant ε_M. The total interaction between ionic species can be written as the sum of hard core (hc) and electrostatic interactions. The hard core interaction between one particle of species i located at $\vec{r}_i$ and a particle of species j located at $\vec{r}_j$ is given by

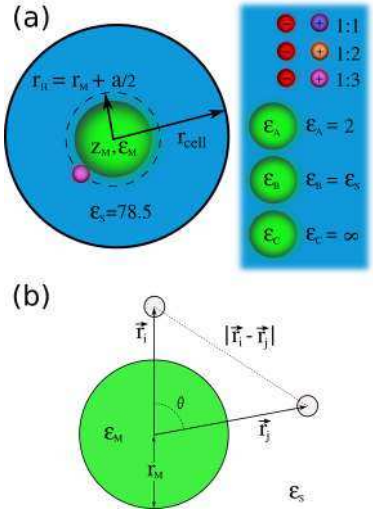

Figure 1. Schematic representation of the model system. The dielectric constant at the interior of the nanoparticle is ε_M. The dielectric constant outside the nanoparticle, ε_S, is the same for the ions and the solvent.

$$u_{hc}(r_{ij}) = \begin{cases} \infty, & \text{if } r_{ij} < \dfrac{d_i + d_j}{2} \\ 0, & \text{if } r_{ij} \geq \dfrac{d_i + d_j}{2} \end{cases} \tag{1}$$

where d_i is the diameter of the ionic species i and $r_{ij} = |\vec{r}_i - \vec{r}_j|$ for i = +, −, M, and j = +, −. The diameter of cations and anions is the same and equal to $d_+ = d_- = a$ = 5 Å. The diameter of the nanoparticle is 10 times the diameter of small ions, i.e., $d_M = 2r_M = 10d_+$ = 50 Å.

The charged nanoparticle is fixed at the center of a spherical hard cell of radius r_{cell}. The electrolyte is confined by a spherical hard cell via a potential

$$u_{cell}(r_i) = \begin{cases} \infty, & \text{if } r_i > r_{cell} - \dfrac{a}{2} \\ 0, & \text{if } r_i \leq r_{cell} - \dfrac{a}{2} \end{cases} \tag{2}$$

Thus, the total hard core energy is zero if all ions are completely enclosed by the spherical hard cell (with no overlaps), and there are no overlaps among all charged particles including the rigid central nanoparticle.

The electrostatic potential produced by a point charge in a solvent of dielectric constant ε_S in the presence of an uncharged spherical nanoparticle of dielectric constant ε_M can be calculated by solving the Poisson equation

$$\nabla^2\phi(\vec{r}) = -\frac{\rho}{\varepsilon_0\varepsilon_S} \tag{3}$$

subject to the continuity of the electrostatic potential and the electric displacement at the dielectric interface, as well as the vanishing of the electrostatic potential at large distances as boundary conditions.[36] From the solution of eq 3, it is possible to write the total energy of N ions around a spherical uncharged nanoparticle in terms of infinite series as[36,19]

$$U_{coul} = \frac{l_{\varepsilon_S}}{2}\sum_{i=1}^{N}\sum_{j=1}^{N}\frac{z_i z_j}{r_{ij}} \quad \text{for } i \neq j \tag{4}$$

dx.doi.org/10.1021/jp5045173 | J. Phys. Chem. B 2014, 118, 8854−8862

$$U_{im} = \frac{l_{\varepsilon_S}}{2}\sum_{i=1}^{N}\sum_{j=1}^{N}(-f)z_i z_j\left\{\sum_{n=0}^{\infty}P_n(\cos\theta)\frac{r_M^{2n+1}}{r_i^{n+1}r_j^{n+1}}\left[1-\frac{1-f}{1-f+2n}\right]\right\} \quad \text{for } i \neq j \tag{5}$$

and

$$U_{si} = \frac{l_{\varepsilon_S}}{2}\sum_{i=1}^{N}(-f)z_i^2\left\{\sum_{n=0}^{\infty}P_n(\cos\theta)\frac{r_M^{2n+1}}{r_i^{2(n+1)}}\left[1-\frac{1-f}{1-f+2n}\right]\right\} \tag{6}$$

where $l_{\varepsilon_S} = (e_0^2)/(4\pi\varepsilon_0\varepsilon_S k_B T)$ is the Bjerrum length in the solvent, e_0 the proton charge, ε_0 the vacuum permittivity, and k_B the Boltzmann constant; P_n are the Legendre polynomials, $f = (\varepsilon_M - \varepsilon_S)/(\varepsilon_M + \varepsilon_S)$, θ is the angle between one particle i located at $\vec{r}_i$ and a particle j located at $\vec{r}_j$, $r_i = |\vec{r}_i|$, $r_j = |\vec{r}_j|$, and $r_{ij} = |\vec{r}_j - \vec{r}_i|$ (see Figure 1b). In analogy to the planar case,[37,38] the term U_{coul} corresponds to the sum of only $1/r$ Coulombic interactions among ions in a single solvent without polarization effects; the term U_{im} represents the sum of interactions among ions and the images of another ions, whereas the term U_{si} is the sum of all self-image ion interactions.

The Gauss law allows us to calculate the electrostatic energy between the nanoparticle and any ion at the interior of the spherical hard cell as

$$U_M = l_{\varepsilon_S}\sum_{i=1}^{N}\frac{z_M z_i}{r_{Mi}} \tag{7}$$

Using the superposition principle, the total electrostatic energy of N ions surrounding a charged nanoparticle in the absence of overlaps (see eqs 1 and 2) can be written as

$$U_{el} = U_{coul} + U_{im} + U_{si} + U_M \tag{8}$$

The infinite series appearing in eqs 4−6 are rapidly convergent, and only 100−200 terms are required to compute them with a reasonable precision in the presence of divalent ions.[19] When the total number of particles increase, this constraint becomes computationally expensive because the calculation of the electrostatic energy scales as N^2. Levin has proposed an analytical approximation that speeds up this kind of calculation significantly.[22] Nonetheless, the dielectric permittivity inside the nanoparticle has to be low to obtain accurate values of the electrostatic energy. Another approximation has been proposed by Cai and collaborators, in which eqs 5 and 6 are reformulated in terms of numerical integrals using a Gauss−Radau quadrature based on Jacobi polynomials.[39] This method has been used in off-lattice simulations,[23] and the explicit expressions used in this work are given in Appendix A.

Monte Carlo (MC) simulations were performed using the standard Metropolis algorithm in the canonical ensemble.[40,41] N_c cations of valence z were added to the main simulation cell in order to satisfy the global electroneutrality condition

$$z_M + \sum_{i=1}^{2}N_i z_i = 0 \tag{9}$$

where z_M is the valence of a negatively charged nanoparticle immersed in a 1:z salt.

The total number of ions varied from 800 to 3200 ions for the 1:z electrolytes. The salt concentration was varied using different radii of the spherical hard cell, r_{cell}, for a fixed number of ions. In the thermalization process, at least 100 000 MC cycles were performed, and between 300 000 to 1 000 000 MC cycles were done to calculate the canonical average.

The ion profiles, $\rho_i(r)$, and radial distribution functions, $g_i(r)$, of ions of species i around the central spherical rigid nanoparticle were calculated as a function of the distance from the simulation data.

The radial distribution functions are defined as

$$g_i(r) = \rho_i(r)/\rho_i(r_{bulk}) \tag{10}$$

where $\rho_i(r_{bulk})$ is the bulk value of the electrolyte at a distance r_{bulk} far away from the central nanoparticle but still inside the spherical hard cell.

The integrated charge is defined as

$$P(r) = z_M + \sum_{j=1}^{2}\int_{r_M}^{r} z_j\rho_j(t)4\pi t^2\,dt \tag{11}$$

which physically represents the net charge of the nanoparticle and the ions contained in a shell of radius r. When $r = r_M$, the integrated charge is $P(r_M) = z_M$ whereas $P(r_{cell}) = 0$ because of the electroneutrality condition.

The mean electrostatic potential can be calculated from

$$\Psi(r) = \frac{e_0}{4\pi\varepsilon_0\varepsilon_S}\int_r^{r_\infty}\frac{P(t)}{t^2}\,dt \tag{12}$$

where $r_\infty \approx r_{bulk}$ is a distance far away from the nanoparticle at which the integrated charge is zero. This distance is used as the reference state of the mean electrostatic potential at which $\Psi(r_{bulk}) \approx 0$.

On the other hand, let us consider a macroscopic multicomponent ionic liquid modeled as an infinite system of charged particles in the three-dimensional space. The radial distribution function of species i can be written formally in terms of the potential of mean force, $W_i(r)$, as[42]

$$g_i(r) = \exp\left(-\frac{W_i(r)}{k_B T}\right) \tag{13}$$

If the potential of mean force, $W_i(r)$, is approximated by the electrostatic work required to bring an ion of species i from infinite to a distance r from a central macroion, that is, $W_i(r) \approx z_i e_0\Psi(r)$, using eqs 11 and 12, it is possible to recast eq 13 as

$$g_i(r) = \exp\left(-z_i l_{\varepsilon_S}\int_r^{r_\infty}\frac{P(t)}{t^2}\,dt\right) \tag{14}$$

which is the integral equation version of the nonlinear Poisson−Boltzmann equation in spherical geometry.[43] This equation satisfies the Poisson equation for the mean electrostatic potential, which vanishes far away from the nanoparticle's surface when $\lim_{r\to\infty}\Psi(r) = 0$, and fulfills the electroneutrality condition for the whole system, $\lim_{r\to\infty}P(r) = 0$, in the thermodynamic limit. Noting that $g_i(r) = \rho_i(r)/\rho_i^{bulk}$ with $\rho_i^{bulk} = \lim_{r\to\infty}\rho_i(r)$, it is easy to see that eq 14 constitutes a set of nonlinear coupled integral equations. These integral equations were solved numerically assuming a Helmholtz plane (or closest approach distance between point-ions and the spherical nanoparticle) equal to $r_H = r_M + a/2$ for the ionic species, and a constant surface charge density at the surface of the nanoparticle $\sigma_0 = (z_M e_0)/(4\pi r_M^2)$. An adaptive Picard scheme

dx.doi.org/10.1021/jp5045173 | J. Phys. Chem. B 2014, 118, 8854−8862

was used to obtain a fast convergence of the nonlinear coupled integral equations defined by eq 14 (see Appendix B).

RESULTS AND DISCUSSION

In analogy to the planar geometry, the Helmholtz plane is defined by a sphere whose radius is the sum of the nanoparticle's radius plus the ionic radius, which is the closest approach distance ($r_H = r_M + a/2$) between the nanoparticle and the ions (see Figure 1a). In Figure 2, the mean electrostatic potential at the Helmholtz plane, Ψ_H, is displayed as a function of the salt concentration for different 1:z electrolytes around a solid spherical nanoparticle. To study the effect of image charges in the electrical double layer, a nanoparticle made of different dielectric materials and valence $z_M = -12$ is considered. In all instances, we observe that the Ψ_H is less negative (the negative nanoparticle is more screened electrostatically) as the dielectric constant of the nanoparticle increases. For the 1:1 electrolyte (displayed in Figure 2a), these differences are small. Nevertheless, when the valence of cations (counterions) increases, they become more evident, as is shown in Figure 2b,c. In the presence of trivalent couterions, a sign inversion of the Ψ_H occurs at high concentrations for the nanoparticle with the highest dielectric constant. In all cases, the nonlinear Poisson–Boltzmann theory predicts a Ψ_H value that is close to the simulation results obtained for a nanoparticle in the absence of image charge effects (i.e., when its dielectric properties correspond to those of water), except for the trivalent cations at low salt concentrations. In Figure 3, we present the effect of increasing the surface charge density of the nanoparticle. Here, we consider a nanoparticle of valence $z_M = -72$ under the same conditions displayed in Figure 2. In this instance, simulation results display the same trends already observed for the lower nanoparticle's valence. Nevertheless, we observe that this time the critical concentration at which the sign of Ψ_H inverts is shifted to lower concentrations. This behavior suggests that the ζ potential and the regime in which the electrophoretic mobility may be inverted could be controlled by choosing nanoparticle materials with appropriate dielectric properties in the presence of multivalent counterions in aqueous solutions. In this regard, we would like to mention that the observed inversion of the mean electrostatic potential occurs, in general, not only at the

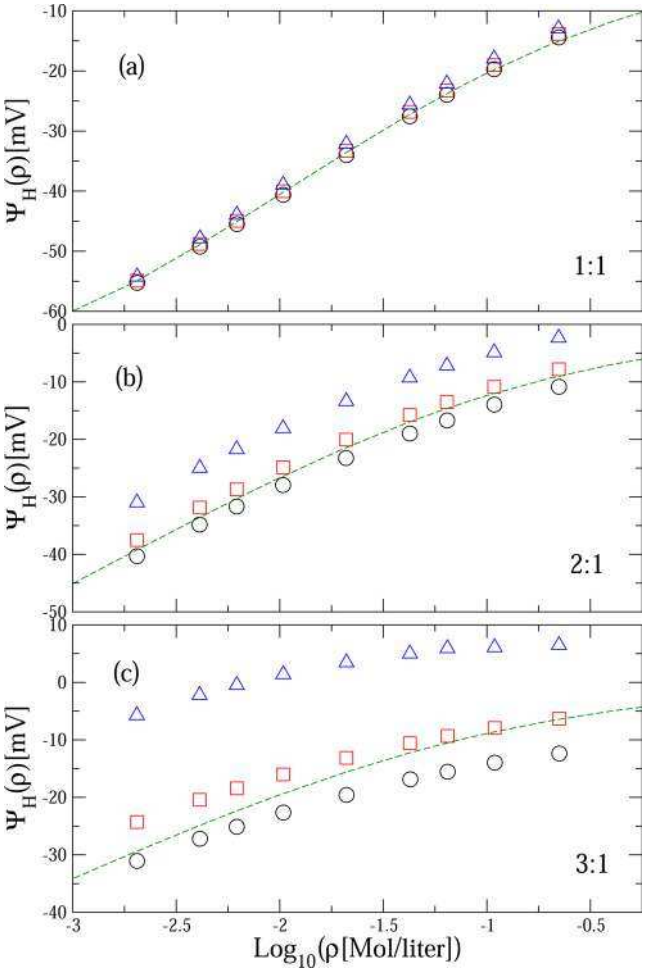

Figure 2. Monte Carlo mean electrostatic potential at the Helmholtz plane around a spherical nanoparticle as a function of the ionic concentration of a 1:z electrolyte. The valence of the nanoparticle is $z_M = -12$. Black circles, red squares, and blue triangles correspond to nanoparticles of dielectric constants 2, 78.5, and ∞, respectively. Here, and in the rest of the figures, the diameter of all ions is $a = 5$ Å, the diameter of the nanoparticle $d_M = 10a = 50$ Å, the dielectric constant of the aqueous solvent $\varepsilon_S = 78.5$, and the temperature of the whole system $T = 298$ K; the error is smaller than the symbol size. Green dashed lines are the theoretical predictions of the nonlinear Poisson–Boltzmann theory with a Stern layer in spherical geometry.

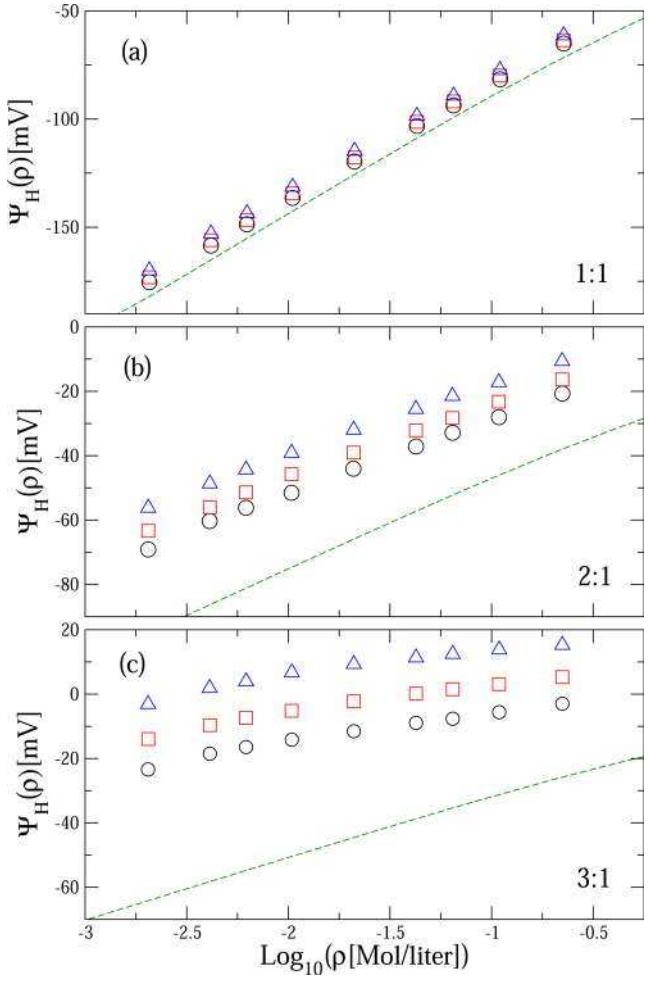

Figure 3. The same as in Figure 2 but for a nanoparticle of valence $z_M = -72$.

dx.doi.org/10.1021/jp5045173 | J. Phys. Chem. B 2014, 118, 8854–8862

Helmoltz plane but also in a region of several ionic radii close to the nanoparticle's surface. As a result, the proposed mechanism for the inversion of the ζ potential and the electrophoretic mobility is expected to be robust regarding the precise location of the shear plane under the current conditions and assumptions of our model system. On the other hand, the nonlinear Poisson−Boltzmann theory predicts values of the mean electrostatic potential that agree qualitatively with simulation data in the absence of polarization effects. Nevertheless, the predictions of this mean field theory deteriorate significantly when the valence of the nanoparticle or counterions augments, and this theoretical approach is unable to predict the sign inversion of Ψ_H at high concentrations in the presence of trivalent ions, as is shown in Figure 3c.

The charge neutralization of the nanoparticle as a function of the distance for different dielectric materials is displayed in Figure 4. The valence of the nanoparticle is $z_M = -12$ for a concentration 0.223 M of 1:z electrolytes. Here, we observe

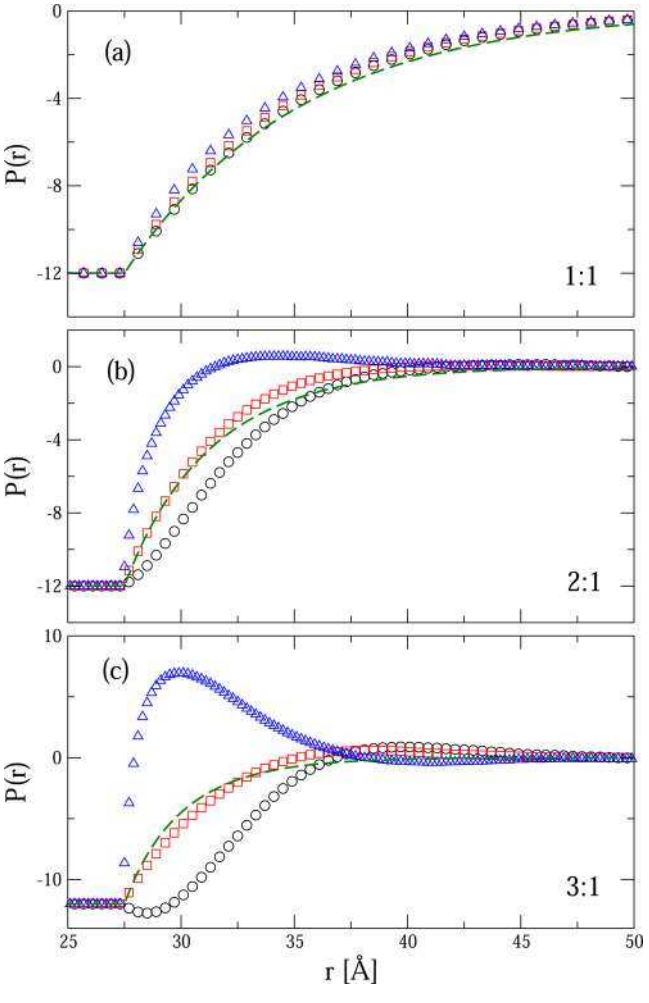

Figure 4. Monte Carlo integrated charge, $P(r)$, as a function of the distance to the center of a spherical nanoparticle, which is immersed in a 0.223 M electrolyte with valences (a) 1:1, (b) 1:2, and (c) 1:3. The valence of the nanoparticle is $z_M = -12$. Black circles, red squares, and blue triangles correspond to nanoparticles of dielectric constants 2, 78.5, and ∞, respectively. Green dashed lines correspond to the theoretical predictions of the nonlinear Poisson−Boltzmann theory with a Stern layer in spherical geometry.

that the net charge of the nanoparticle as a function of the distance (characterized by the integrated charge, $P(r)$) is less negative near the nanoparticle's surface as a function of the dielectric permittivity of the nanoparticle. For the 1:1 electrolyte, the charge neutralization is similar for the different dielectric materials. In the presence of divalent cations, the integrated charge profiles are well-separated. Here, we observe that $P(r,\varepsilon) > P(r,\varepsilon')$ for all r if $\varepsilon > \varepsilon'$, where ε and ε' represent different values of the dielectric constant of a charged nanoparticle immersed in a divalent electrolyte. Physically, this means that the charge neutralization is higher for higher dielectric permittivities of the nanoparticle. In addition, the integrated charge also displays a sign inversion, or the so-called charge reversal,[44] for the material with the highest dielectric constant. In the case of trivalent cations, the differences in the integrated charge profiles already displayed by divalent cations are more conspicuous. We still observe that $P(r,\varepsilon) > P(r,\varepsilon')$ if $\varepsilon > \varepsilon'$, but now only in a smaller region close to the nanoparticle's surface. For the material with the highest dielectric constant, we observe that the magnitude of the maximum charge reversal is more than half the magnitude of the original bare charge. For the material with the lowest dielectric permittivity, we observe that very close to the nanoparticle's surface the magnitude of the integrated charge can be larger than the native bare charge, that is, $|P(r)| > |z_M|$ as is illustrated in Figure 4c. The adsorption of like-charged ions on the nanoparticle's surface increasing locally its net charge is the so-called surface charge amplification.[44,45] In this case, the surface charge amplification of a small dielectric nanoparticle is driven by the appearance of a strong ionic exclusion produced by polarization effects, even in the presence of size symmetric ions, as we will show below. The integrated charges obtained via the nonlinear Poisson−Boltzmann theory are close to simulation data in the absence of polarization effects, which is consistent with the behavior of the Ψ_H displayed in Figure 2.

To understand the differences of the integrated charge profiles displayed in Figure 4, we show the corresponding ionic profiles for divalent and trivalent counterions in water. In Figure 5, the radial distribution functions, $g_j(r)$, for divalent cations are plotted as a function of the distance. Here, we observe that for the lowest dielectric permittivity the divalent counterions display a strong repulsive interaction with the nanoparticle. As a result, divalent counterions display a maximum beyond the Helmholtz plane (i.e., the distance of closest approach between ions and the nanoparticle). In the absence of polarization effects (i.e., when the dielectric properties of the nanoparticle and water are the same), the contact value of both ionic species at the Helmholtz plane increases in comparison to that of the previous case. As cations are the counterions of the negative nanoparticle, they are preferentially adsorbed because of electrostatic interactions. For the material with highest dielectric constant, the adsorption of both ionic species is further enhanced. This behavior can be explained qualitatively in terms of the self-energy of one point charge immersed in a macroscopic medium in front of another medium with larger dielectric permittivity. In particular, let us consider a sharp interface between the two different dielectric media in planar geometry. The self-energy of a charged point particle in these conditions is given by[37]

$$u_{self} = -\frac{\varepsilon_2 - \varepsilon_1}{\varepsilon_2 + \varepsilon_1}\frac{e_0^2}{4\pi\varepsilon_0\varepsilon_1}\frac{z^2}{x} \qquad (15)$$

dx.doi.org/10.1021/jp5045173 | J. Phys. Chem. B 2014, 118, 8854−8862

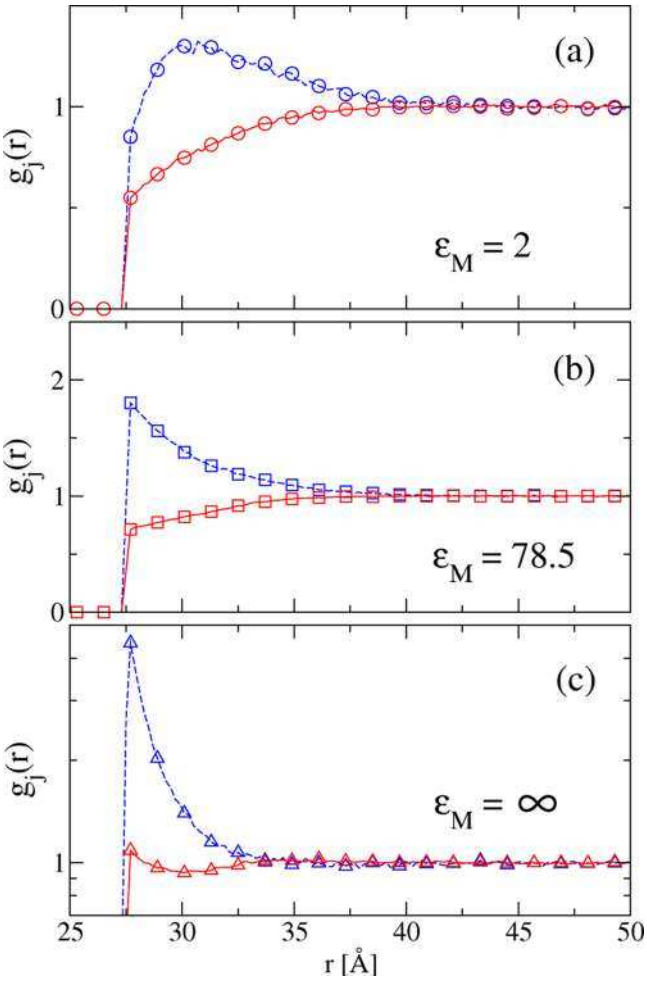

Figure 5. Monte Carlo radial distribution functions, $g_j(r)$, as a function of the distance to the center of a spherical nanoparticle, which is immersed in a 1:2 electrolyte at an ionic concentration of 0.223 M. The valence of the nanoparticle is $z_M = -12$. Circles, squares, and triangles correspond to nanoparticles of dielectric constants (a) 2, (b) 78.5, and (c) ∞, respectively. Dashed and solid lines are guides to the eye associated with divalent counterions and monovalent co-ions, respectively.

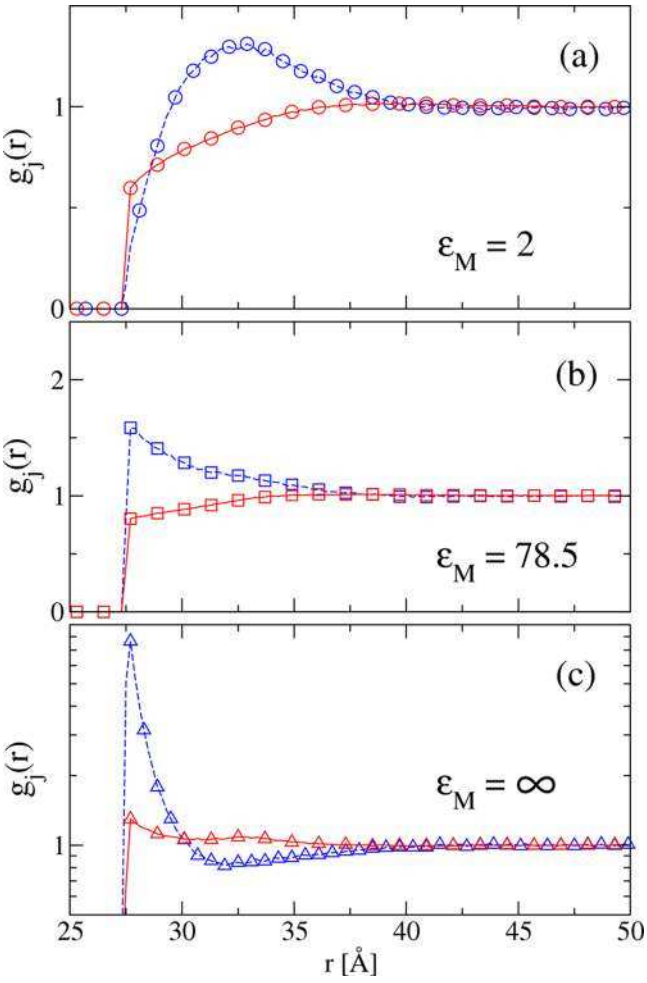

Figure 6. The same as in Figure 5 but for a 1:3 electrolyte.

where x is the perpendicular distance from the dielectric discontinuity to the position of a point charge of valence z (or charge ze_0), ε_1 the dielectric constant of the medium in which the charged particle is located, and ε_2 the dielectric constant of the other dielectric medium (e.g., a colloidal particle). As a result, if $\varepsilon_2 < \varepsilon_1$, then the ionic self-energy is positive. This can be associated with a repulsive interaction between the charged particle and the dielectric interface. On the contrary, if $\varepsilon_2 > \varepsilon_1$, then the ionic self-energy is negative and the interaction between the charged particle and the dielectric interface becomes attractive. Quantitatively, these effects are enhanced when the interactions with the images of other charges due to the spherical dielectric discontinuity are taken into account according to eq 5. In addition, notice that the magnitude of the self-energy of a charged point particle grows as the square of its valence. Thus, the behavior observed in the case of divalent ions should be exacerbated for the trivalent cations. This is precisely what is observed in Figure 6, in which the radial distribution functions for trivalent counterions are plotted as a function of the distance. In Figure 6a we observe that the maximum displayed by trivalent cations is shifted far away from the nanoparticle's surface in comparison with the case of divalent cations under similar conditions (see Figure 5a). Moreover, we see that the adsorption of trivalent counterions can be lower than the adsorption of monovalent co-ions very close to the nanoparticle's surface. A very interesting consequence is that monovalent co-ions can increase the magnitude of the native charge of the nanoparticle, as is shown in Figure 4c. This phenomenon is the so-called surface charge amplification, which has been comprehensively studied in spherical geometry in the absence of polarization effects in previous studies.[44,45] In those works, we showed that the ionic size asymmetry of ions and excluded volume effects can promote a preferential adsorption of small ions to weakly charged colloidal particles at high electrolyte concentrations. In the presence of polarization effects, repulsive image charge contributions can promote the exclusion of ions from the region that is located very close to the nanoparticle's surface. This exclusion can be significantly stronger for multivalent counterions regarding monovalent co-ions. As a result, the charge asymmetry of equally sized 1:z electrolytes may induce the appearance of the surface charge amplification by promoting a preferential adsorption of monovalent co-ions to the nanoparticle's surface, increasing locally the nanoparticle's net charge. The occurrence of the surface charge amplification due to polarization effects also has been observed by Wang and Ma near an infinite planar wall in the presence of mixed electrolytes,[46] which is consistent with our simulation results in

dx.doi.org/10.1021/jp5045173 | J. Phys. Chem. B 2014, 118, 8854−8862

spherical geometry. On the other hand, regarding the material with the highest dielectric constant displayed in Figure 6c, we observe that the contact values of both ionic species increase significantly in comparison to the divalent instance displayed in Figure 5c. Another significant difference is the appearance of a spatial region where the role of co-ions and counterions is interchanged, which is the so-called charge inversion.[47,44] This charge inversion produces the sign inversion of the corresponding mean electrostatic potential at the Helmholtz plane already displayed in Figure 2c.

CONCLUSIONS

We have studied the role of polarization effects in the charge neutralization and electrostatic screening of a solid spherical nanoparticle made of different materials immersed in a 1:z aqueous electrolyte. The role of the salt concentration as well as the surface charge density of the nanoparticle have been also analyzed via Monte Carlo simulations and the nonlinear Poisson−Boltzmann theory in spherical geometry. In general, we observe that the charge neutralization and electrostatic screening of the charged nanoparticle near its surface augments as a function of its dielectric permittivity. For weakly charged nanoparticles, different dielectric materials produce small differences in the electrical double layer of 1:1 salts. In contrast, the structural and macroscopic properties of the electrical double layer for divalent and trivalent counterions display a stronger dependence on the dielectric properties of the nanoparticle. Several authors have proposed that the colloidal surface charge density is closely related to the regimes in which the sign of the mean electrostatic potential at the Helmholtz plane can be inverted by multivalent ions.[48,49] Our results display the same trend. However, our simulations also suggest that the ζ potential and the regime in which the electrophoretic mobility of a nanoparticle may be inverted by multivalent counterions could be controlled by the dielectric properties of the suspended nanoparticles in aqueous solvents.

Our numerical simulations display a short-range repulsion between ions and a weakly charged nanoparticle with low dielectric permittivity due to polarization effects. These repulsive image charge interactions promote the exclusion of ions from a region that is located very close to the nanoparticle's surface. We have shown that this ionic exclusion can be significantly stronger for multivalent counterions regarding monovalent co-ions with the same ionic size. As a result, the charge asymmetry of 1:z electrolytes may induce the phenomenon of surface charge amplification, i.e., the adsorption of like-charged ions on the nanoparticle's surface increasing locally its net charge. This phenomenon has been also observed in the presence of a size-asymmetric salt around a weakly charged nanoparticle without polarization effects.[44,45] In both scenarios, we have shown that the appearance of an exclusion region of counterions, due to steric or image charge effects, may induce a preferential adsorption of co-ions promoting the surface charge amplification of the nanoparticle.

On the other hand, the electrostatic screened charge of small nanoparticles at large separation distances, or the so-called renormalized charge, plays a fundamental role in the stability regimes and kinetics of aggregation of colloidal solutions.[50−52] In a recent study, we have shown that the classical Derjaguin−Landau−Verwey−Overbeek (DLVO) theory is unable to predict the rich phenomenology displayed by highly charged nanoparticles suspended in a monovalent supporting electrolyte even in the absence of polarization effects.[53] In that study, it was estimated theoretically that polarization effects were small for hydrated monovalent salts, which is in agreement with the simulation results of the mean electrostatic potential at the Helmholtz plane presented here.

As an extension of the present work, we mention that in the presence of multivalent aqueous electrolytes or molecular solvent with structure,[54,55] polarization effects may be significant depending on the difference of the dielectric properties between the solvent and solutes. The impact of polarization effects in the renormalized charge of small nanoparticles in the presence of multivalent ions can be determined using a versatile numerical method developed recently in our group.[56] This scheme includes the exact bridge functions that are crucial at short distances from computer simulations and recovers the corresponding asymptotic Yukawa potential at large separation distances, which may be significantly different from that predicted by the classical DLVO theory.[53]

APPENDIX A

As has been shown by Cai and collaborators,[39] eqs 5 and 6 can be recast as

$$U_{\mathrm{im}} = \frac{l_{\varepsilon_1}}{2}\sum_{i=1}^{N}\sum_{j=1}^{N} z_i z_j I(\vec{r}_i, \vec{r}_j) \quad \text{for } i \neq j \tag{16}$$

and

$$U_{\mathrm{si}} = \frac{l_{\varepsilon_1}}{2}\sum_{i=1}^{N} z_i^2 I(\vec{r}_i, \vec{r}_i) \tag{17}$$

where

$$I(\vec{r}_i, \vec{r}_j) = \frac{(-f + e w_0)\lambda_i}{|\vec{r}_j - \lambda_i \vec{r}_i|} + \sum_{m=1}^{M} \frac{e w_m \lambda_i}{\left|\vec{r}_j - \left(\frac{\lambda_i^2}{c_m}\right)\vec{r}_i\right|} \tag{18}$$

$$f = \frac{\varepsilon_M - \varepsilon_S}{\varepsilon_M + \varepsilon_S} \tag{19}$$

$$e = f(1-f)\tau \times 2^{\left(\frac{f-1}{2}\right)\tau - 1} \tag{20}$$

$$\tau = \frac{2}{1-f} \tag{21}$$

$$\lambda_i = \frac{r_M}{|\vec{r}_i|} \tag{22}$$

$$c_m = \left(\frac{2}{1 - S_m}\right)^{\tau} \tag{23}$$

S_m and w_m for $m = 0,...M$, are the Jacobi−Gauss−Radau points and weights such that the Jacobi polynomials are orthogonal under an appropriate weight on the interval $[-1,1]$.[39,57,58] We have observed that $M = 10$ terms is an optimal number to maintain a good balance between efficiency and accuracy for the simulated systems, in agreement with Gan and Xu.[23]

APPENDIX B

Let us define

$$g_i(r) = K_i[g_1(r), g_2(r)] \tag{24}$$

dx.doi.org/10.1021/jp5045173 | J. Phys. Chem. B 2014, 118, 8854−8862

for $r \geq r_M + a/2$ as an abbreviated form of eq 14. If we discretize the distance to the center of the nanoparticle as $r_j = j\Delta r$, where Δr is a small distance in comparison to the ionic size, it is possible to define

$$g_i^{new}(r_j) = K_i[g_1^{old}(r_j), g_2^{old}(r_j)] \quad (25)$$

The accuracy of the numerical solution can be imposed by requiring that $\gamma < \gamma_0$, where

$$\gamma = \sum_{i=1}^{2} \sum_{j} (g_i^{new}(r_j) - g_i^{old}(r_j)) \quad (26)$$

and γ_0 is a small finite number. According to the classical Piccard method, a new approximation to the solution of eq 24 can be written as

$$g_i^{new'}(r_j) = (1 - \alpha)g_i^{old}(r_j) + \alpha g_i^{new}(r_j) \quad (27)$$

and

$$g_i^{old}(r_j) = g_i^{new'}(r_j) \quad (28)$$

if $K_i[g_1^{old}(r_j), g_2^{old}(r_j)]$ corresponds to a numerical finite value and α is a constant number. Large values of α may trap the numerical solution in a local minimum and tiny values of α are time-consuming. Thus, we propose the following prescription to update adaptively the value of α: if $\gamma_{new} < \gamma_{old}$ then $\alpha = 1.1\alpha$, otherwise $\alpha = 1/\alpha$. In this way, even if the starting α is minute, it takes only a few tens of iterations to increase an order of magnitude because the growth of α is exponential. If the error increases, the magnitude of α is decreased at a similar rate.

AUTHOR INFORMATION

Corresponding Author

*E-mail: m-olvera@northwestern.edu.

Notes

The authors declare no competing financial interest.

ACKNOWLEDGMENTS

We thank Pedro González-Mozuelos and Enrique González-Tovar for valuable discussions and insightful suggestions. This work, including the computer cluster where part of the simulations were performed, was funded by the Office of the Director of Defense Research and Engineering (DDR&E) and the Air Force Office of Scientific Research (AFOSR) under Award FA9550-10-1-0167. This research was supported in part through the computational resources and staff contributions provided for the Quest high performance computing facility at Northwestern University, which is jointly supported by the Office of the Provost, the Office for Research, and Northwestern University Information Technology.

REFERENCES

(1) Fumagalli, L.; Esteban-Ferrer, D.; Cuervo, A.; Carrascosa, J. L.; Gomila, G. Label-free Identification of Single Dielectric Nanoparticles and Viruses with Ultraweak Polarization Forces. *Nat. Mater.* **2012**, *11*, 808−816.

(2) Gomila, G.; Esteban-Ferrer, D.; Fumagalli, L. Quantification of the Dielectric Constant of Single Non-spherical Nanoparticles from Polarization Forces: Eccentricity Effects. *Nanotechnology* **2013**, *24*, 505713.

(3) Mottaghizadeh, A.; Lang, P. L.; Cui, L. M.; Lesueur, J.; Li, J.; Zheng, D. N.; Rebuttini, V.; Pinna, N.; Zimmers, A.; Aubin, H. Nanoparticles Charge Response from Electrostatic Force Microscopy. *Appl. Phys. Lett.* **2013**, *102*, 053118.

(4) Maheshwari, V.; Kane, J.; Saraf, R. F. Self-Assembly of a Micrometers-Long One-dimensional Network of Cemented Au Nanoparticles. *Adv. Mater. (Weinheim, Ger.)* **2008**, *20*, 284−287.

(5) Dilger, J. P.; McLaughlin, S. G. A.; McIntosh, J. T.; Simon, S. A. The Dielectric Constant of Phospholipid Bilayers and the Permeability of Membranes to Ions. *Science* **1979**, *206*, 1196−1198.

(6) Gurnev, P. A.; Bezrukov, S. M. Inversion of Membrane Surface Charge by Trivalent Cations Probed with a Cation-Selective Channel. *Langmuir* **2012**, *28*, 15824−15830.

(7) Gramse, G.; Dols-Perez, A.; Edwards, M. A.; Fumagalli, L.; Gomila, G. Nanoscale Measurement of the Dielectric Constant of Supported Lipid Bilayers in Aqueous Solutions with Electrostatic Force Microscopy. *Biophys. J.* **2013**, *104*, 1257−1262.

(8) Warshel, A.; Sharma, P. K.; Kato, M.; Parson, W. W. Modeling electrostatic effects in proteins. *Biochim. Biophys. Acta* **2006**, *1764*, 1647−1676.

(9) Onsager, L.; Samaras, N. T. T. The Surface Tension of Debye-Hückel Electrolytes. *J. Chem. Phys.* **1934**, *2*, 528−536.

(10) Ben-Yaakov, D.; Andelman, D.; Podgornik, R.; Harries, D. Ion-specific Hydration Effects: Extending the Poisson-Boltzmann Theory. *Curr. Opin. Colloid Interface Sci.* **2011**, *16*, 542−550.

(11) Hatlo, M. M.; van Roij, R.; Lue, L. The electric double layer at high surface potentials: The influence of excess ion polarizability. *Europhys. Lett.* **2012**, *97*, 28010.

(12) Démery, V.; Dean, D. S.; Podgornik, R. Electrostatic interactions mediated by polarizable counterions: Weak and strong coupling limits. *J. Chem. Phys.* **2012**, *137*, 174903.

(13) Naji, A.; Kanduč, M.; Forsman, J.; Podgornik, R. Perspective: Coulomb fluids—Weak coupling, strong coupling, in between and beyond. *J. Chem. Phys.* **2013**, *139*, 150901.

(14) Bell, G. M.; Levine, S. Electrical Forces between Uncharged Plates in Ionic Solutions. *J. Chem. Phys.* **1968**, *49*, 4584−4599.

(15) Kjellander, R.; Marčelja, S. Electrolyte Solutions between Uncharged Walls. *Chem. Phys. Lett.* **1987**, *142*, 485−491.

(16) Kanduč, M.; Naji, A.; Forsman, J.; Podgornik, R. Attraction between Neutral Dielectrics Mediated by Multivalent Ions in an Asymmetric Ionic Fluid. *J. Chem. Phys.* **2012**, *137*, 174704.

(17) Zwanikken, J. W.; Olvera de la Cruz, M. Tunable Soft Structure in Charged Fluids Confined by Dielectric Interfaces. *Proc. Natl. Acad. Sci. U.S.A.* **2013**, *110*, 5301−5308.

(18) Linse, P. Image Charge Effects in Spherical Symmetry with Applications to Micellar Systems. *J. Phys. Chem.* **1986**, *90*, 6821−6828.

(19) Messina, R. Image Charges in Spherical Geometry: Application to Colloidal Systems. *J. Chem. Phys.* **2002**, *117*, 11062.

(20) Lue, L.; Linse, P. Macroion Solutions in the Cell Model Studied by Field Theory and Monte Carlo Simulations. *J. Chem. Phys.* **2011**, *135*, 224508.

(21) dos Santos, A. P.; Bakhshandeh, A.; Levin, Y. Effects of the Dielectric Discontinuity on the Counterion Distribution in a Colloidal Suspension. *J. Chem. Phys.* **2011**, *135*, 044124.

(22) Bakhshandeh, A.; dos Santos, A. P.; Levin, Y. Weak and Strong Coupling Theories for Polarizable Colloids and Nanoparticles. *Phys. Rev. Lett.* **2011**, *107*, 107801.

(23) Gan, Z.; Xu, Z. Multiple-image Treatment of Induced Charges in Monte Carlo Simulations of Electrolytes near a Spherical Dielectric Interface. *Phys. Rev. E: Stat., Nonlinear, Soft Matter Phys.* **2011**, *84*, 016705.

(24) Vega-Acosta, J. R.; Cadena-Nava, R. D.; Gelbart, W. M.; Knobler, C. M.; Ruiz-García, J. Electrophoretic Mobilities of a Viral Capsid, Its Capsid Protein, and Their Relation to Viral Assembly. *J. Phys. Chem. B* **2014**, *118*, 1984−1989.

(25) Iwata, N.; Neves, M. A.; Watanabe, J.; Sato, S.; Ichikawa, S. Stability Control of Large Oil Droplets by Layer-by-layer Deposition Using Polyelectrolyte Dietary Fibers. *Colloids Surf., A* **2014**, *440*, 2−9.

(26) Gillespie, D. A. J.; Hallett, J. E.; Elujoba, O.; Che Hamzah, A. F.; Richardson, R. M.; Bartlett, P. Counterion Condensation on Spheres in the Salt-free Limit. *Soft Matter* **2014**, *10*, 566.

(27) Wu, Y.; Li, Q.; Deng, F.; Liang, X.; Liu, H. Solvent Effect on ζ Potential at an Aqueous/Oil Interface in Surfactant-Free Emulsion. *Langmuir* **2014**, *30*, 1926−1931.
(28) Preočanin, T.; Šupljika, F.; Lovrak, M.; Barun, J.; Kallay, N. Bubbling Potential as a Measure of the Charge of Gas Bubbles in Aqueous Environment. *Colloids Surf., A* **2014**, *443*, 129−134.
(29) Hunter, R. J. *Foundations of Colloid Science*; Clarendon Press: Oxford, U.K., 1987.
(30) Hunter, R. J. *Zeta Potential in Colloid Science*; Academic Press: San Diego, CA, 1981.
(31) Lozada-Cassou, M.; González-Tovar, E.; Olivares, W. Nonlinear Effects in the Electrophoresis of a Spherical Colloidal Particle. *Phys. Rev. E: Stat., Nonlinear, Soft Matter* **1999**, *60*, R17−R20.
(32) Lozada-Cassou, M.; González-Tovar, E. Primitive Model Electrophoresis. *J. Colloid Interface Sci.* **2001**, *239*, 285−295.
(33) Ramos, J.; Forcada, J.; Hidalgo-Alvarez, R. Cationic Polymer Nanoparticles and Nanogels: From Synthesis to Biotechnological Applications. *Chem. Rev. (Washington, DC, U.S.)* **2014**, *114*, 367−428.
(34) Hühn, D.; Kantner, K.; Geidel, C.; Brandholt, S.; De Cock, I.; Soenen, S. J. H.; Rivera Gil, P.; Montenegro, J. M.; Braeckmans, K.; Müllen, K.; Ulrich Nienhaus, G.; Klapper, M.; Parak, W. J. Polymer-Coated Nanoparticles Interacting with Proteins and Cells: Focusing on the Sign of the Net Charge. *ACS Nano* **2013**, *7*, 3253−3263.
(35) Palberg, T.; Schweinfurth, H.; Köller, T.; Müller, H.; Schöpe, H. J.; Reinmüller, A. Structure and Transport Properties of Charged Sphere Suspensions in (Local) Electric Fields. *Eur. Phys. J.: Spec. Top.* **2013**, *222*, 2835−2853.
(36) Böttcher, C. J. F. *Theory of Electric Polarization*; Elsevier: New York, 1973.
(37) Jackson, J. D. *Classical Electrodynamics*, 3rd ed.; John Wiley & Sons: New York, 2001.
(38) Torrie, G. M.; Valleau, J. P. Double Layer Structure at the Interface between Two Immiscible Electrolyte Solutions. *J. Electroanal. Chem.* **1986**, *206*, 69−79.
(39) Cai, W.; Deng, S.; Jacobs, D. Extending the Fast Multipole Method to Charges Inside or Outside a Dielectric Sphere. *J. Comput. Phys.* **2007**, *223*, 846−864.
(40) Allen, M. P.; Tildesley, D. J. *Computer Simulation of Liquids*; Oxford University Press: New York, 1989.
(41) Frenkel, D.; Smit, B. *Understanding Molecular Simulation*; Academic Press: London, 2002.
(42) McQuarrie, D. A. Statistical Mechanics; University Science Books: Sausalito, CA, 2000.
(43) Guerrero-García, G. I.; Gonzalez-Tovar, E.; Chávez-Páez, M. Simulational and Theoretical Study of the Spherical Electrical Double Layer for a Size-Asymmetric Electrolyte: The Case of Big Coions. *Phys. Rev. E: Stat., Nonlinear, Soft Matter* **2009**, *80*, 021501.
(44) Guerrero-García, G. I.; González-Tovar, E.; Olvera de la Cruz, M. Effects of the Ionic Size-asymmetry around a Charged Nanoparticle: Unequal Charge Neutralization and Electrostatic Screening. *Soft Matter* **2010**, *6*, 2056−2065.
(45) Guerrero-García, G. I.; González-Tovar, E.; Olvera de la Cruz, M. Entropic Effects in the Electric Double Layer of Model Colloids with Size-asymmetric Monovalent Ions. *J. Chem. Phys.* **2011**, *135*, 054701.
(46) Wang, Z.-Y.; Ma, Y.-Q. Computational Evidence of Two Driving Mechanisms for Overcharging in an Electric Double Layer Near the Point of Zero Charge. *Phys. Rev. E: Stat., Nonlinear, Soft Matter* **2012**, *85*, 062501.
(47) Greberg, H.; Kjellander, R. Charge Inversion in Electric Double Layers and Effects of Different Sizes for Counterions and Coions. *J. Chem. Phys.* **1998**, *108*, 2940−2953.
(48) Diehl, A.; Levin, Y. Smoluchowski Equation and the Colloidal Charge Reversal. *J. Chem. Phys.* **2006**, *125*, 054902.
(49) Martín-Molina, A.; Rodríguez-Beas, C.; Hidalgo-Álvarez, R.; Quesada-Pérez, M. Effect of Surface Charge on Colloidal Charge Reversal. *J. Phys. Chem. B* **2009**, *113*, 6834−6839.
(50) Verwey, E. J. W.; Overbeek, J. T. G. *Theory of the Stability of Lyophobic Colloids*; Elsevier: New York, 1948.
(51) Russel, W. B.; Saville, D. A.; Schowalter, W. R. *Colloidal Dispersions*; Cambridge University Press: Cambridge, U.K., 1989.
(52) Sonntag, H.; Strenge, K. *Coagulation Kinetics and Structure Formation*; Plenum Press: New York, 1987.
(53) Guerrero-García, G. I.; González-Mozuelos, P.; Olvera de la Cruz, M. Large Counterions Boost the Solubility and Renormalized Charge of Suspended Nanoparticles. *ACS Nano* **2013**, *7*, 9714−9723.
(54) González-Mozuelos, P.; Olvera de la Cruz, M. Solvent and Nonlinear Effects on the Charge Renormalization of Nanoparticles within a Molecular Electrolyte Model. *Physica A* **2008**, *387*, 5362−5370.
(55) González-Mozuelos, P.; Olvera de la Cruz, M. Asymmetric Charge Renormalization for Nanoparticles in Aqueous Media. *Phys. Rev. E: Stat., Nonlinear, Soft Matter* **2009**, *79*, 031901.
(56) González-Mozuelos, P.; Guerrero-García, G. I.; Olvera de la Cruz, M. An exact method to obtain effective electrostatic interactions from computer simulations: The case of effective charge amplification. *J. Chem. Phys.* **2013**, *139*, 064709.
(57) Gautschi, W. *Orthogonal Polynomials Computation and Approximation*; Oxford University Press: New York, 2004.
(58) Gautschi, W. Algorithm 726: ORTHPOL—A package of routines for generating orthogonal polynomials and Gauss-type quadrature rules. *ACM Trans. Math Soft.* **1994**, *20*, 21−62.